

TPS50601-SP Single-Event Effects Summary

The effect of heavy-ion irradiation on the single-event effect performance of the TPS50601-SP point-of-load switching regulator has been summarized in this report. Heavy-ions with LET_{EFF} ranging from 48.5 to 94.0 MeV-cm²/mg were used to irradiate production devices in hundreds of experiments with fluences ranging from 1×10^6 to 1×10^7 ions/cm² per run, over a variety of input and output voltages, and load conditions across temperature. The results demonstrate that the TPS50601-SP, when operated within its “safe operating area,” is SEB-free, SEL-free and nearly SET-free under all conditions. The TPS50601-SP has a low SEFI (self-recoverable) saturation cross-section under maximum load and input/output voltage.

Contents

1	Overview	3
2	Single-Event Effects	4
3	Test Device and Evaluation Board Information	6
4	Irradiation Facility and Setup	7
5	Depth, Range, and LET_{EFF} Calculation	9
6	Test Set-Up and Procedures	10
7	Safe-Operating-Area (SOA) Results	12
8	Single Event Latch-up (SEL) Results	13
9	SEFI Results	14
10	SET Results	19
11	Event Rate Calculations	22
12	Summary	23
Appendix A	Total Ionizing Dose from SEE Experiments	24
Appendix B	Orbital Environment Estimations	25
Appendix C	Confidence Interval Calculations	27
Appendix D	References	29

List of Figures

1	Photo of Delidded TPS50601-SP (left) and a Pin-Out Diagram (right)	6
2	TPS50601SPEVM, 6-A/12-A, SWIFT™ Regulator Evaluation Module Board Top-View (left) and Bottom-View (right)	6
3	Photo of the TPS50601-SP Evaluation Board Mounted in Front of the Heavy-Ion Beam Exit Port	8
4	Generalized Cross-Section of the LBC7 Technology BEOL Stack on the TPS50601-SP (left) and GUI of RADsim Application Used to Determine Key Ion Parameters (right)	9
5	Block Diagram of SEE Test Set-Up With the TPS50601-SP	11
6	SOA Curves for the TPS50601-SP	12
7	V_{OUT} Overlay of 200 Events Demonstrating SEFI 1, SEFI 2 and SETs in TPS50601-SP	14
8	P_{GOOD} Overlay of 200 Events Demonstrating SEFI 1, SEFI 2 in TPS50601-SP	15
9	DPO Waveform Captures of V_{OUT} Overlay of 62 SEFI 2 Events in a TPS50601-SP	16
10	DPO Waveform Captures of P_{GOOD} Overlay of 62 SEFI 2 Events in a TPS50601-SP	16
11	DPO Waveform Captures of Soft-Start (SS) Pin Response Overlay	17
12	DPO Waveform Captures of Phase (PH) Pin Overlay	17
13	SEFI Cross-Section vs LET_{EFF} for TPS50601-SP	18
14	The Worst-Case SET Events Captured by PXI	19
15	SET Histogram of Number of Events vs SET Magnitude (ΔV_{OUT})	20
16	Cross-Section of SET events $V_o > 5\%$ vs LET_{EFF} for TPS50601-SP	21

17	Integral Particle Flux vs LET_{EFF}	25
18	Device Cross-Section vs LET_{EFF}	26

List of Tables

1	Overview Information	3
2	Silver and Praseodymium Ion LET_{EFF} , Depth, and Range in Silicon	9
3	Equipment Set and Parameters Used for the SEE Testing the TPS50601-SP	10
4	Summary of TPS50601-SP SEL Results	13
5	Weibull Fitting Parameters for the SEFI Data	18
6	Weibull Fitting Parameters for SET Data	21
7	SEL Event Rate Calculations for Worst-Week LEO and GEO Orbits	22
8	SEFI 2 Event Rate Calculations for Worst-Week LEO and GEO Orbits	22
9	SET Event Rate Calculations for Worst-Week LEO and GEO Orbits	22
10	Experimental Example Calculation of Mean-Fluence-to-Failure (MFTF) and σ Using a 95% Confidence Interval	28

Trademarks

All trademarks are the property of their respective owners.

1 Overview

The TPS50601-SP is a space-grade, radiation hardened, 6.3-V, 6-A synchronous buck point-of-load (POL) converter, which has been optimized for small designs with its high-efficiency operation and integration of the high-side and low-side power MOSFETs into a compact monolithic solution providing the smallest footprint in the industry. Further space saving is achieved through current mode control, which reduces component count while providing a high switching frequency for reduced inductor size. The device is offered in a thermally enhanced 20-pin ceramic, dual in-line flat-pack package. General device information and test conditions are listed in [Table 1](#).

For more detailed technical specifications, user-guides, application notes please go to: www.ti.com/product/TPS50601-SP.

Table 1. Overview Information

DESCRIPTION	DEVICE INFORMATION
TI Part Number	TPS50601-SP
Orderable Name	5962R1022101VSC
Device Function	Point-of-Load (POL) Switching Regulator
Technology	250-nm Linear BiCMOS
Exposure Facility	Radiation Effects Facility, Cyclotron Institute, Texas A&M University
Heavy-Ion Fluence per Run	$1 \times 10^6 - 1 \times 10^7$ ions/cm ²
Irradiation Temperature	25°C and 125°C (For SEL Testing)

2 Single-Event Effects

The primary concern for the TPS50601-SP are its resilience against the destructive single event effects (DSEE): single event burn-out (SEB) and single-event latch-up (SEL). The TPS50601-SP is NOT sensitive to SEB as long as it is operated within the safe-operating-area (SOA) where it has been verified to be SEB-free with heavy-ions of LET_{eff} of up to 94.0 MeV-cm²/mg at room temperature and $T = 125^{\circ}\text{C}$ (though SEB susceptibility has been shown to decrease with increasing temperature [1][2] so the majority of SEB tests were performed at room temperature). For the TPS50601-SP operating within the SOA the potential for SEB is eliminated.

The TPS50601-SP was also characterized for SEL events. In mixed technologies such as the Linear BiCMOS 7 process used for the TPS750601-SP, the presence of CMOS circuitry introduces a potential SEL susceptibility. SEL can occur if excess current injection caused by the passage of an energetic ion is high enough to trigger the formation of a parasitic cross-coupled PNP and NPN bipolar structure (formed between the p-substrate and n-well and n+ and p+ contacts) [3][4]. If formed, the parasitic bipolar structure creates a high-conductance path (creating a steady-state current that is orders-of-magnitude higher than the normal operating current) between power and ground that persists (is "latched") until power is removed or until the device is destroyed by the high-current state. For the design of the TPS50601-SP, SEL-susceptibility was reduced by maximizing anode-cathode spacing (tap spacing) while increasing the number of well and substrate ties in the CMOS portions of the layout to minimize well and substrate resistance effects. Additionally, junction isolation techniques were used – with buried wells and guard ring structures isolating the CMOS p- and n-wells [5][6][7]. The design techniques applied for SEL-mitigation were sufficient as the TPS50601-SP exhibited absolutely no SEL with heavy-ions of up to $LET_{eff} = 94.0$ MeV-cm²/mg at fluences in excess of 10^7 ions/cm² and a die temperature of 125°C .

Under heavy-ions, the TPS50601-SP exhibits three transient modes that are fully recoverable without the need for external intervention. One is a single-event functional interrupt (SEFI) in the P_{GOOD} control logic inducing a brief ($\sim 80 \mu\text{s}$) P_{GOOD} transition to occur even though the output voltage is stable (false P_{GOOD} signal). We call this mode SEFI 1. It does NOT interrupt the regulated power output, and no soft-start is initiated, as it is only the P_{GOOD} signal itself that is affected. Since SEFI 1 creates a very narrow pulse on P_{GOOD} , the event can be filtered by a use of a properly sized capacitor on P_{GOOD} without significantly impacting the operation for valid P_{GOOD} transitions. The other type of SEFI, SEFI 2, occurs when a heavy-ion event induces an single event transient (SET) in the output voltage, momentarily reducing the output voltage significantly below its regulated value. During a SEFI 2 event, the TPS50601-SP produces a low on P_{GOOD} and a soft-start is initiated. Soft-start is determined by an external capacitor charged by an internal current and the main purpose is to avoid inrush currents. (www.ti.com/product/TPS50601-SP)

Ultimately, after each of the hundreds of SEFI 2 events observed, the part goes into soft restart and fully recovers in less than 6 ms (with $C_{SS} = 10 \text{ nF}$) to a properly regulated output voltage with P_{GOOD} restored to a high level indicating that V_{OUT} is good. SEFI 2 is fully self-recovering and does NOT require any external reset or mitigation.

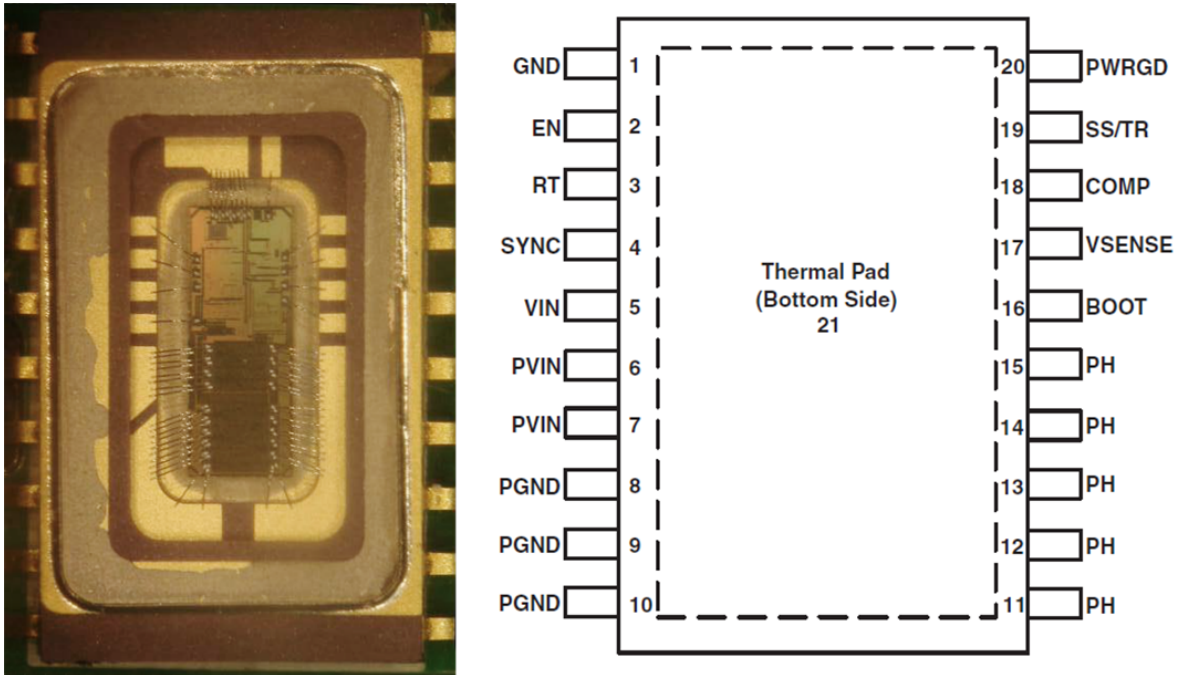
Any event that causes a change in the output voltage exceeding $\sim \pm 9\%$ forces the P_{GOOD} signal low. P_{GOOD} is designed to protect down-stream components from power outages by providing a warning that the voltage output is no longer regulated. During heavy ion SEE testing, P_{GOOD} transitions were logged as SEFIs, while events that cause output excursions of less than $\pm 9\%$ were logged as SETs. Given the large output capacitance (660 μF), SET were expected to be rare. Indeed, during extensive testing at effective LET of 48.5 to 56.4 MeV-cm²/mg NO SETs were observed under any condition with a trigger set to capture SETs where V_{OUT} dropped by 4% or more. At an effective LET of 65.7 MeV-cm²/mg, we saw a few events of $\sim 5\%$. At an effective LET of 86.5 MeV-cm²/mg, SETs were more common and while most were 5% or lower, a few were as high as 8%.

A combination of several different techniques to suppress SET and SEFI were used in the design of the TPS50601-SP POL. Among these mitigation techniques were the use triple redundant logic circuits [8], time constant adjustment [9], a new architectural circuit design and special isolation techniques to prevent latch-up induced by heavy-ions. The efficacy of these techniques was verified by using a custom heavy-ion charge injection model in SPICE, developed specifically for this junction isolated BiCMOS technology, iteratively applied as the design was modified. This model was initially developed on theoretical calculations by taking into account specific parameters from the process technology like depletion region depths for different components and doping profiles. The model was then modified based on real heavy-ion measurements. Once adjusted, this model was used to design the different circuit blocks within the TPS50601-SP POL. The initial model used in SPICE was implemented as a double-exponential function but it was simplified to a piecewise-linear function to accelerate simulation time [10][11].

Triple-redundant logic with majority voting was used in critical high-speed logic circuit blocks within the TPS50601-SP. This reduced the probability of SEFI in sensitive logic. Time-constant adjustment was implemented in digital logic that is not speed-sensitive and in analog circuit blocks. This design technique consisted of reducing on-state series resistance ($R_{DS(on)}$) of sensitive transistors, increasing storage capacitance in sensitive nodes and increasing biasing currents in analog functions like the band-gap reference and error amplifier. A heavy-ion induced SET in the output transistors and error amplifier can result in missing pulses, runt pulses, or wide pulses at the PWM circuit output, which can produce voltage droop or transients at the output of the power converter. A new design technique was implemented in the TPS50601-SP to significantly reduce the recovery time of the output if the converter ever experiences a missing pulse due to a high-energy heavy-ion strike in the state machine. The idea is to sense such an event very quickly in the analog domain (error amplifier) and adjust the duty-cycle accordingly. Therefore the output of the converter is stable against a large majority of SETs. This innovation also enables reliable performance with a smaller output capacitor that results in board area savings and in an overall smaller solution.

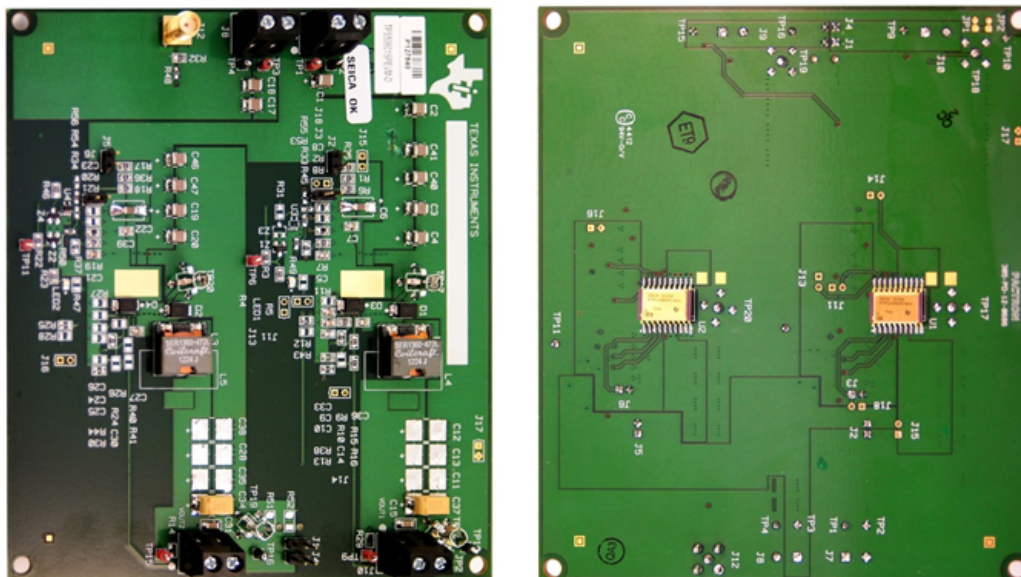
3 Test Device and Evaluation Board Information

The TPS50601-SP is packaged in a 20-pin thermally-enhanced dual ceramic flat pack package (HKH) as shown in Figure 1. The TPS50601SPEVM-D (dual unit) evaluation board was used to evaluate the performance and characteristics of the TPS50601-SP. Top and bottom views of the evaluation board used for radiation testing are shown in Figure 2. Only a single unit was tested during each run in the ion beam experiments. For more information about the evaluation board please go to www.ti.com/product/TPS50601-SP/technicaldocuments.



(1) The package lid was removed to reveal the die face for all heavy-ion testing.

Figure 1. Photo of Delidded TPS50601-SP (left) and a Pin-Out Diagram (right)



(1) The TPS50601-SP is mounted on the bottom side.

Figure 2. TPS50601SPEVM, 6-A/12-A, SWIFT™ Regulator Evaluation Module Board Top-View (left) and Bottom-View (right)

4 Irradiation Facility and Setup

The heavy-ion species used for the SEE studies on this product were provided and delivered by the TAMU Cyclotron Radiation Effects Facility [10] using a superconducting cyclotron and advanced electron cyclotron resonance (ECR) ion source. At the fluxes used, ion beams had good flux stability and high irradiation uniformity over a 1-in diameter circular cross sectional area for the in-air station. Uniformity is achieved by means of magnetic defocusing. The flux of the beam is regulated over a broad range spanning several orders of magnitude. For the bulk of these studies ion fluxes between 10^4 and 10^5 ions/sec-cm² were used to provide heavy-ion fluences between 10^6 and 10^7 ions/cm². SEE responses were checked for event rate linearity (as a function of increasing flux) over the range used for the experiments. Linearity was confirmed, thus total number of events was related directly to the fluence of the tests independent of the flux used for a particular test. **This confirmation is important since the ion beam flux is so much more highly accelerated than the actual space environment heavy-ion fluxes – thus we wanted to be sure not to over-predict sensitivity due to double multiple simultaneous hits to redundant protection circuits.**

In addition to hundreds of runs with dozens of devices/boards, the data reported in this report was based on finalized EVM boards with optimized component values that follow datasheet and application note recommendations. For these final experiments, Silver (Ag) ions were used at angles of 0°, 30°, and 45° for LET_{EFF} of 48.5, 56.4, and 70.0 MeV-cm²/mg respectively. Praseodymium (Pr) ions were also used, at angles of 0°, 30°, 40°, 45° for a LET_{EFF} of 65.7, 76.2, 86.5 and 94.0 MeV-cm²/mg respectively. The Ag and Pr ions used had a total kinetic energy of 1.634 GeV and 2.114 GeV, respectively, in the vacuum (15-MeV/amu line). Ion beam uniformity for all tests was in the range of 92% to 99%.

The TPS50601-SP test board used for the experiments at the TAMU facility is shown in [Figure 3](#). The board was also rotated 90° for some of the experiments to check for the possibility of different sensitivities due to asymmetric layouts. The 1-in diameter ion beam port is in the middle of the photo (partially occluded by the TPS50601-SP PCB). The beam port has a 1-mil Aramica® window to allow in-air testing while maintaining the vacuum within the accelerator with only minor ion energy loss. Note that the de-lidded TPS50601-SP device-under-test is mounted on the opposite side of the EVM board for beam testing. The air space between the device and the ion beam port window was maintained at 40 mm for all runs.

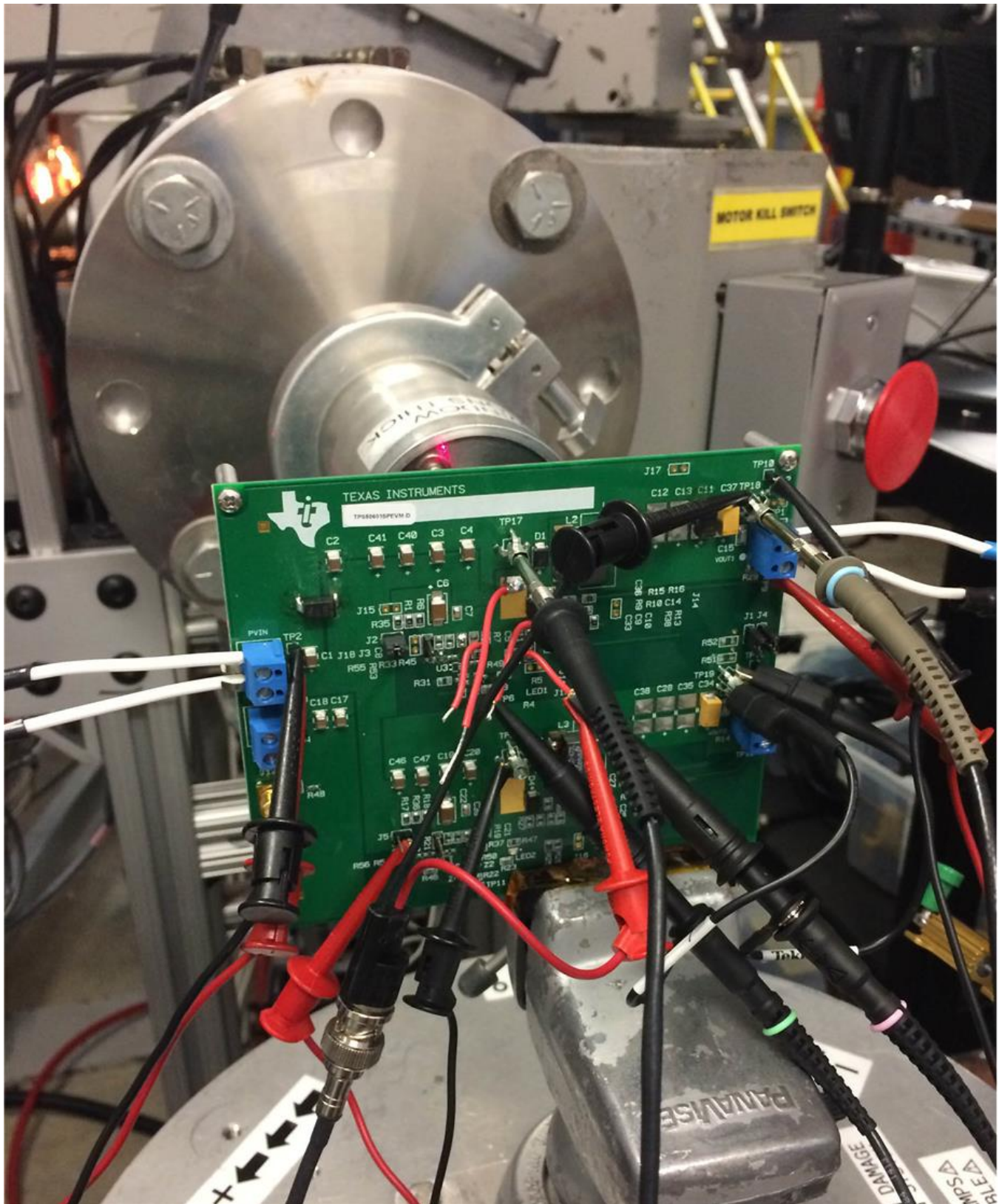


Figure 3. Photo of the TPS50601-SP Evaluation Board Mounted in Front of the Heavy-Ion Beam Exit Port

5 Depth, Range, and LET_{EFF} Calculation

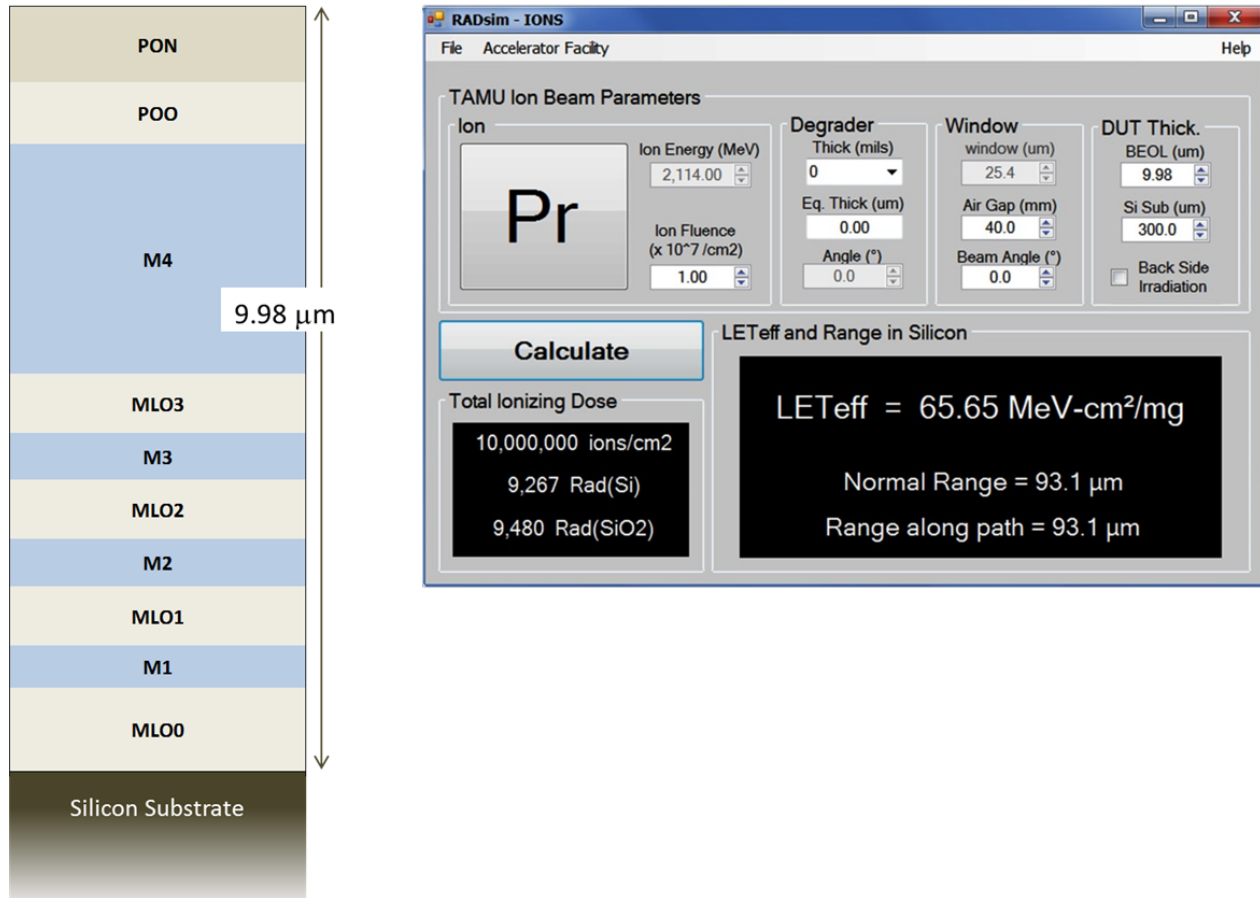


Figure 4. Generalized Cross-Section of the LBC7 Technology BEOL Stack on the TPS50601-SP (left) and GUI of RADsim Application Used to Determine Key Ion Parameters (right)

The TPS50601-SP is fabricated in the TI Linear BiCMOS 250-nm process with a back-end-of-line (BEOL) stack consisting of three levels of standard thickness aluminum metal on a 0.6-μm pitch, and a 4th level of thick aluminum. The total stack height from the surface of the passivation to the silicon surface is 9.98 μm based on nominal layer thickness as shown in . No polyimide or other coating was present so the uppermost layer was the nitride passivation layer (PON). Accounting for energy loss through the 1-mil thick Aramica (Kevlar®) beam port window, the 40-mm air gap, and the BEOL stack over the TPS50601-SP, the effective LET (LET_{EFF}) at the surface of the silicon substrate and the depth and ion range was determined with the custom RADsim-IONS application (developed at Texas Instruments and based on the latest SRIM2013 [11] models). The results are shown in Table 2. The stack was modeled as a homogeneous layer of silicon dioxide (valid since SiO₂ and aluminum density is similar).

Table 2. Silver and Praseodymium Ion LET_{EFF}, Depth, and Range in Silicon

ION TYPE	ANGLE OF INCIDENCE	DEPTH IN SILICON (μm)	RANGE IN SILICON (μm)	LET _{EFF} (MeV-cm ² /mg)	NOTES
Ag	0°	87.8	87.8	48.46	For latest tests
Ag	30°	74.7	86.3	56.35	For latest tests
Ag	45°	59.1	83.6	69.95	
Pr	0°	93.1	93.1	65.65	For latest tests
Pr	30°	79.2	91.5	76.17	
Pr	40°	68.9	89.9	86.52	For latest tests
Pr	45°	62.8	88.8	93.98	For SEL

6 Test Set-Up and Procedures

SEE testing was performed on a TPS50601-SP device mounted on a TPS50601SPEVM-D, 6-A/12-A, Regulator Evaluation Module. The device was provided power to the PVIN input on the J7 terminal block using the N6702 precision power supply in a 4-wire configuration. The PVIN and V_{IN} were tied together using the J2 jumper on the EVM. In the last series of tests for this report, the device was loaded using a discrete power resistor of $0.4\ \Omega$ in order to obtain a load current of 6.225 A at $V_{OUT} = 2.49\ V$.

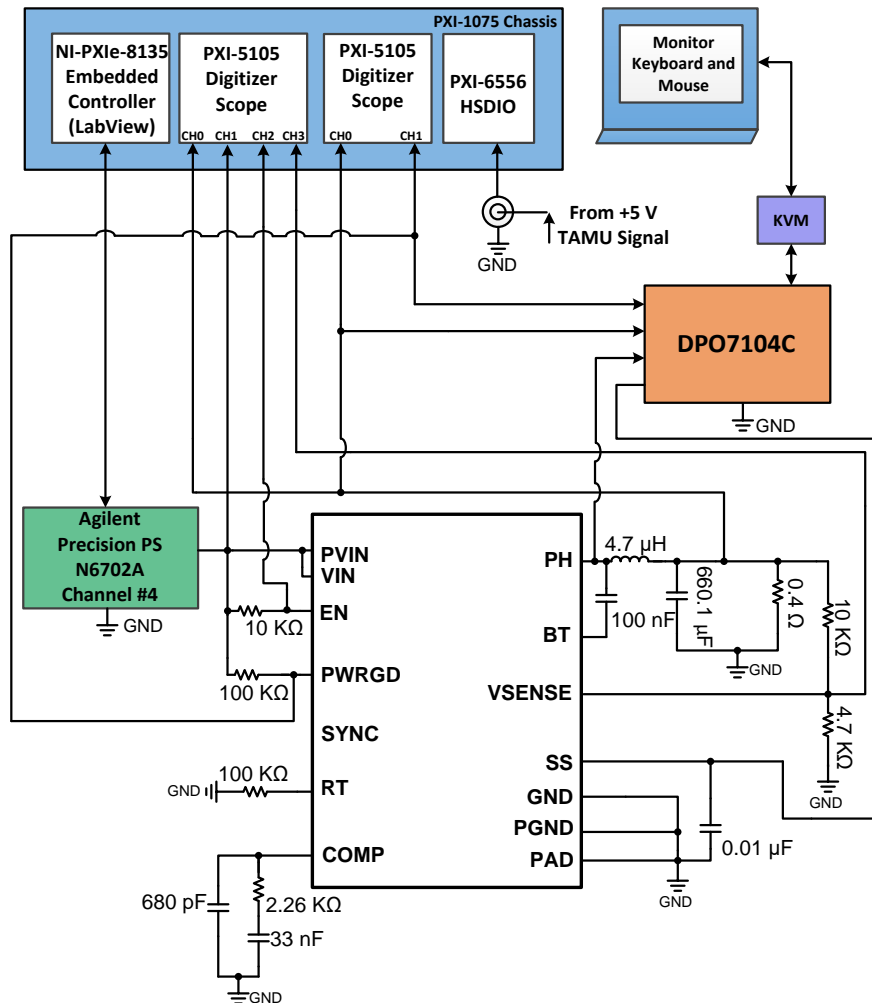
The SEE events were monitored using two National Instruments (NI) PXIe 5105 (60 MS/s and 60 MHz of bandwidth) digitizer modules and one Tektronix DPO7104C Digital Phosphor Oscilloscope (DPO) with 4 channels of 40 GS/s and 2.5 GHz of bandwidth. The DPO was used to monitor the Soft Start (SS), Phase (PH), V_{OUT} and P_{GOOD} signals and was triggered from the SS using a negative edge trigger. The first NI-PXIe Scope card (#1) was used to monitor V_{OUT} , V_{IN} , V_{SENSE} and Enable and was triggered from V_{OUT} using an edge negative trigger set at 1 V. The second NI-PXIe Scope card (#2) was used to monitor P_{GOOD} and V_{OUT} and was triggered from P_{GOOD} using an edge negative trigger. With the exception of the DPO digital oscilloscope, all equipment was controlled and monitored using a custom-developed LabVIEW® program (PXi-RadTest) running on a NI-PXIe-8135 Controller. A block diagram of the set-up used for SEE testing the TPS50601-SP is illustrated in Figure 5 and the connections, limits and compliances used are shown in Table 3. In general, the TPS50601-SP was tested at room temperature (no external heating applied) where the die temperature was usually $\sim 40^{\circ}\text{C}$ to 45°C under maximum load conditions. A die temperature of 125°C was used for SEL testing and was achieved with a convection heat gun aimed at the die. The die temperature was monitored during the testing using a K-Type thermocouple attached to the heat slug of the package with thermal paste. Since the package is designed to dissipate heat by conduction the die temperature is within a few degrees of room temperature even under full load conditions unless external heat is applied.

Table 3. Equipment Set and Parameters Used for the SEE Testing the TPS50601-SP

PI NAME	EQUIPMENT USED	CAPABILITY	COMPLIANCE	RANGE OF VALUES USED
P_{VIN}/V_{IN}	Agilent N6702A (Ch # 4)	5 A	5 A	5 V
Oscilloscope Card	HSDIO NI-PXIe 5105	60 MS/s	—	20 MS/s
Digital Oscilloscope	Tektronix DPO7104C	40 GS/s	—	20 MS/s
Digital I/O	NI PXIe 6556	200 MHz	—	50 MHz

All boards used for SEE testing were fully checked for functionality and dry runs performed to ensure that the test system was stable under all bias and load conditions prior to being taken to the TAMU facility. During the heavy-ion testing, the LabView control program powered up the TPS50601-SP device and set the external sourcing and monitoring functions of the external equipment. After functionality and stability had been confirmed, the beam shutter was opened to expose the device to the heavy-ion beam. The shutter remained open until the target fluence was achieved (determined by external detectors and counters).

During irradiation the PXIe-5101 scope card continuously monitored the Soft Start, Phase, V_{OUT} and P_{GOOD} outputs of the TPS50601-SP with any changes on the V_{OUT} output going below 1 V (at V_{out} or P_{GOOD}) triggering a capture. During a trigger event, the digital scope card would capture



(1) TPS50601-SP mounted on a TPS50601SPEVM-D, 6-A/12-A, Regulator Evaluation Module

Figure 5. Block Diagram of SEE Test Set-Up With the TPS50601-SP

50k samples (the card was continuously digitizing so when triggered, a predefined 20% of the samples that preceded the event were stored). The NI scope cards captured events lasting up to 2.5 ms (50k samples at 20 MS/s). In parallel, the DPO monitored Soft Start, Phase, V_{OUT} and P_{GOOD} triggering from Soft Start using a negative edge at 1 V. The Sample rate was set to 20 MS/s with a much longer capture window of 10 ms and recording 20% or (2 ms) before the event. The DPO was set to fast frame during the test, under this configuration the scope had a 3.2- μ s update rate. The DPO enabled captured of the events and full soft-start recovery cycle of the TPS50601-SP POL. In addition to monitoring the voltage levels of the two scopes and one DPO, the current on the P_{VIN}/V_{IN} pin was also monitored during each test to enable separation of SEFI induced state changes from those caused by the occurrence of an SEL event. No sudden increases in current were observed (outside of normal fluctuations) on any of the test runs indicated that no SEL events occurred during the hundreds of tests run. The signature for SETs was expected to be voltage excursions of less than $\pm 9\%$ of the output amplitude on the V_{OUT} pin (the magnitude of all SET events was extracted from the capture data in post-processing). SETs causing variations larger than $\pm 9\%$ always invoked a P_{GOOD} signal and were considered SEFIs for this evaluation.

7 Safe-Operating-Area (SOA) Results

A large number of TPS50601-SP devices were deliberately operated at maximum load (6 A) while V_{IN} was increased with each subsequent run over the full range of LET_{EFF} until a SEB was observed. The purpose was to define at what voltages and loads the onset of SEB was observed. Even at the maximum LET_{EFF} tested (94.0 MeV-cm²/mg) no SEB events were observed at voltages at 5 V with load currents at 6 A. The TPS50601-SP maximum load current capability is 6 A.

With PVIN voltage increased above 5 V there is increased risk of SEB. The result of several hundred runs with fluences from 10⁶ – 10⁷ ions/cm² is shown in Figure 6. SEB failures are denoted as red symbols. The cross-section for these events is extremely small since over many dozens of tests only single SEB events were observed. The green points are summaries of multiple runs where no SEB event was ever observed.

The green area represents the SOA for the TPS50601-SP POL where no SEB was observed for any ion LET_{EFF} . The yellow and orange areas denote load conditions where the onset of SEB was observed. The red area represents voltage and load conditions that are unsafe due to the potential for destructive SEB events.

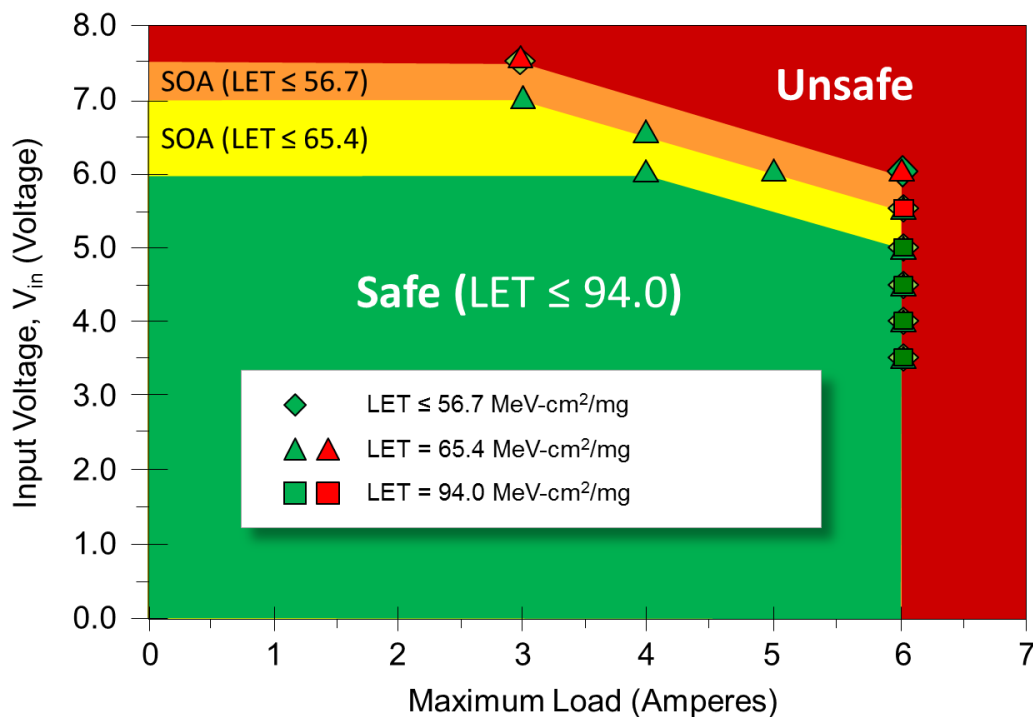


Figure 6. SOA Curves for the TPS50601-SP

8 Single Event Latch-up (SEL) Results

All SEL characterizations were performed with forced hot air to maintain the die temperature at 125°C during the tests. The device was exposed to a Praseodymium (Pr) heavy-ion beam incident on the die surface at 45° for an effective LET of 94.0 MeV-cm²/mg. A total fluence of 10⁷ ions/cm² was used in all runs. Run duration to achieve this fluence was approximately 2 minutes. The SEL results are summarized in [Table 4](#). No SEL events were observed under any of the test runs over any of the input voltage and load conditions, indicating that the TPS50601-SP is SEL-immune at T = 125°C and LET = 94 MeV-cm²/mg.

Table 4. Summary of TPS50601-SP SEL Results⁽¹⁾⁽²⁾

RUN #	DEV #	Temp (°C)	ION TYPE	INCIDENT ANGLE (°)	FLUENCE (ions/cm ²)	V _{IN} (V)	V _O (V)	LOAD (A)	SEL EVENTS
29	3B	125	Pr	45	1.0 × 10 ⁷	5.5	2.5	4.0	0
30	3B	125	Pr	45	1.0 × 10 ⁷	6.0	2.5	4.0	0
32	4A	125	Pr	45	1.0 × 10 ⁷	5.0	2.5	5.3	0
33	4A	125	Pr	45	1.0 × 10 ⁷	5.5	2.5	5.3	0
34	4A	125	Pr	45	1.0 × 10 ⁷	5.0	2.5	6.0	0

⁽¹⁾ SEL results with T = 125°C and LET_{EFF} = 93.98 MeV-cm²/mg.

⁽²⁾ No SEL events were observed for any of the runs under the full range of load conditions.

Upper-bound SEL cross-sections for a single condition (σ_{SEL1}) and over all bias and load conditions (σ_{SELALL}) were calculated based on 0 events observed using a 95% confidence interval (see [Appendix C](#) for discussion of confidence limits):

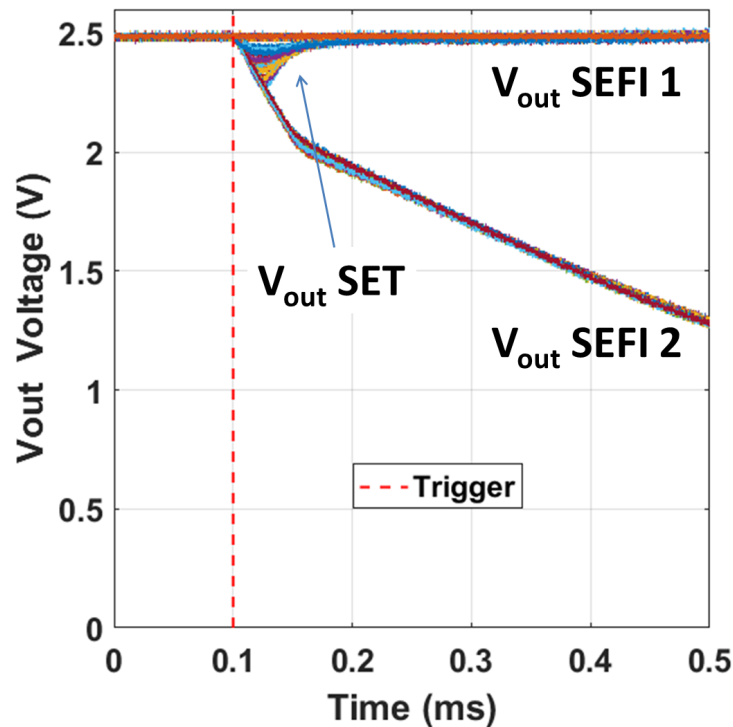
$$\sigma_{\text{SEL1}} \leq 3.69 \times 10^{-7} \text{ cm}^2/\text{device LET} = 94.0 \text{ MeV-cm}^2/\text{mg, T} = 125^\circ\text{C, 95\% conf.} \quad (1)$$

$$\sigma_{\text{SELALL}} \leq 7.38 \times 10^{-8} \text{ cm}^2/\text{device LET} = 94.0 \text{ MeV-cm}^2/\text{mg, T} = 125^\circ\text{C, 95\% conf.} \quad (2)$$

9 SEFI Results

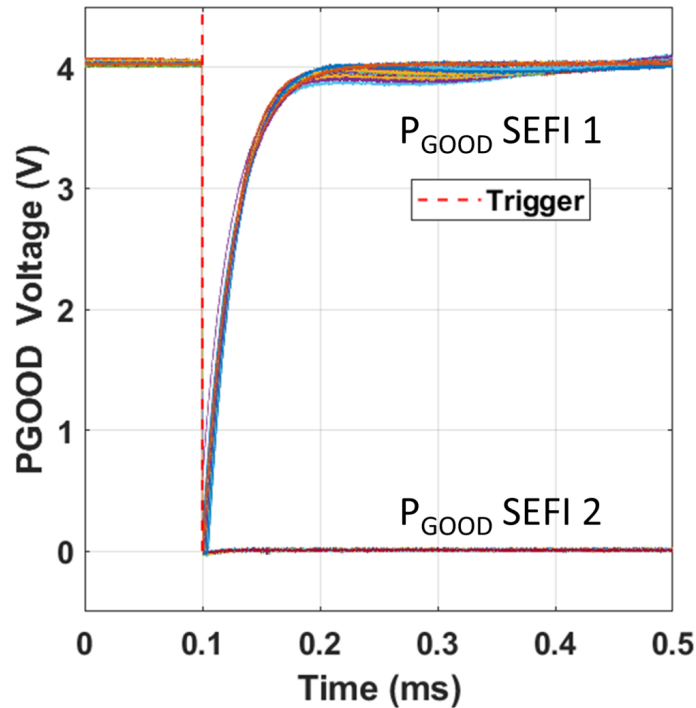
In the case of the TPS50601-SP, SEFIs were categorized as heavy-ion-induced events that could affect down-stream system power. Two distinct types of SEFI events were observed: SEFI 1 events were caused by a heavy-ion disturbance only in the P_{GOOD} control logic such that it would generate a brief but erroneous P_{GOOD} transition while V_{OUT} was unaffected by the event. In contrast, SEFI 2 events caused an actual disruption of the regulated V_{OUT} with a valid P_{GOOD} transition and a soft-start recovery after each event.

The previously described PXI digitizer was used to capture both SEFI 1 and 2 types, while the DPO, with its larger memory was used to capture the entire response from SEFI 2 events to capture the full recovery of the TPS50601-SP. Overlays of all V_{OUT} and P_{GOOD} waveforms captured by the PXI during an exposure of 10^7 ions/cm² heavy ions with an LET of 86.5 MeV-cm²/mg is shown in Figure 7 and Figure 8 respectively. SEFI 1 events are characterized by a short-lived (< 70 μ s) P_{GOOD} transient. Since V_{OUT} is unaffected during a SEFI 1 event, the erroneous P_{GOOD} glitch can be attenuated with a filter on the P_{GOOD} pin, effectively mitigating any down-stream effect of SEFI 1.



- (1) $V_{IN} = 5.0$ V, $V_{OUT} = 2.5$ V, and load of 6 A during exposure to 10^7 ions/cm² of $LET_{EFF} = 86.5$ MeV-cm²/mg.
- (2) Output voltage is unaffected and fully regulated during SEFI 1.

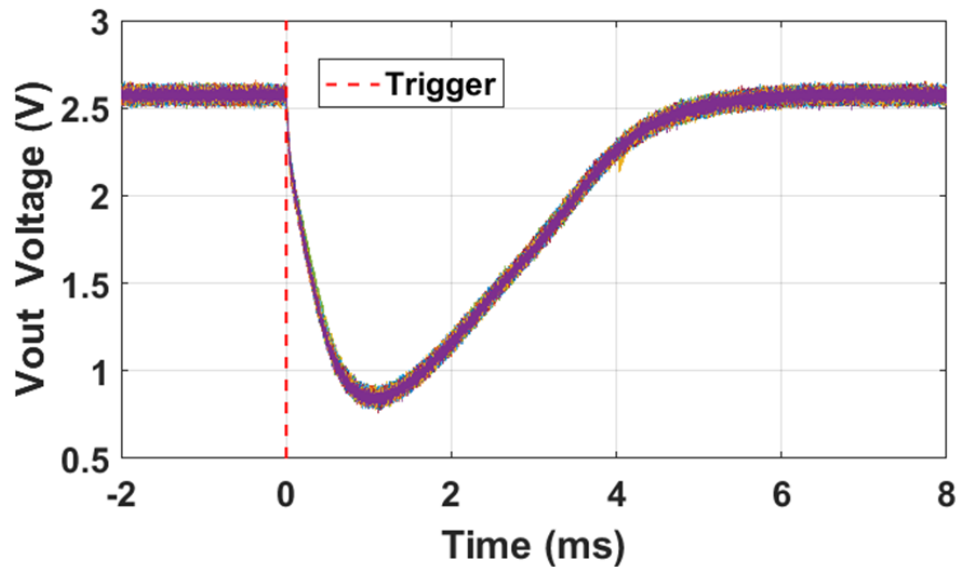
Figure 7. V_{OUT} Overlay of 200 Events Demonstrating SEFI 1, SEFI 2 and SETs in TPS50601-SP



(1) $V_{IN} = 5.0\text{ V}$, $V_{OUT} = 2.5\text{ V}$, and load of 6 A during exposure to 10^7 ions/cm^2 of $LET_{EFF} = 86.5\text{ MeV-cm}^2/\text{mg}$.

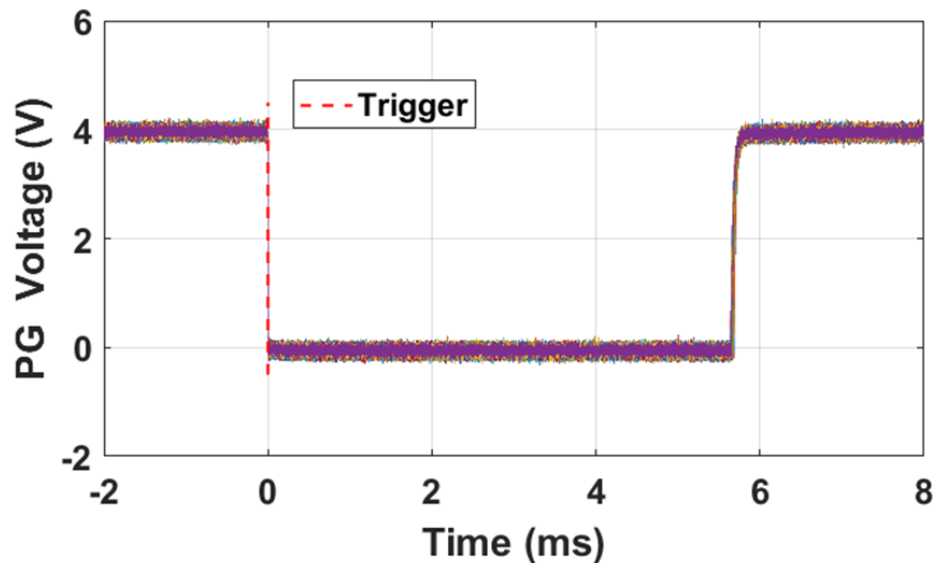
Figure 8. P_{GOOD} Overlay of 200 Events Demonstrating SEFI 1, SEFI 2 in TPS50601-SP

In addition to the PXI digitizer channels, a DPO was also used to capture V_{OUT} , P_{GOOD} , Soft Start, and Phase outputs for every SEFI 2 event that occurred – an example of this data is shown in [Figure 9](#), [Figure 10](#), [Figure 11](#), and [Figure 12](#). These were captured during each SEFI 2 event observed during an exposure of 10^7 ions/cm^2 with an LET_{EFF} of $86.5\text{ MeV-cm}^2/\text{mg}$. Since the DPO triggered off of the Soft Start (SS) pin, only SEFI 2 type events were captured (SEFI 1 did NOT trigger a soft start as V_{OUT} was unaffected). Due to the DPO's larger buffer, the entire waveform for each signal was captured for each of the 62 events, demonstrating how TPS50601-SP self-recovers from SEFI 2 events, going into soft start and getting back to a fully regulated output after each event. For all of the SEFI 2 events, the V_{OUT} dropped significantly, down to about 15-20% of the original V_{OUT} value within 1 ms, but V_{OUT} automatically recovered back to a regulated output within < 6 ms. Note that after about 5.7 ms the P_{GOOD} returns to a high value, signaling that V_{OUT} is within the target regulated range. This SEFI 2 response was virtually identical over hundreds of runs and for 5 different LET conditions, thus the observed V_{OUT} transient is independent of the actual details of the ion event itself and dominated by the circuit response dynamics. The recovery time-constant is set by the C_{SS} capacitor connected to the SS/TR pin. For this experiment, C_{SS} was 10 nF, which would correspond to a rise time of about 4 ms assuming a typical I_{SS} of $\sim 2\text{ }\mu\text{A}$.



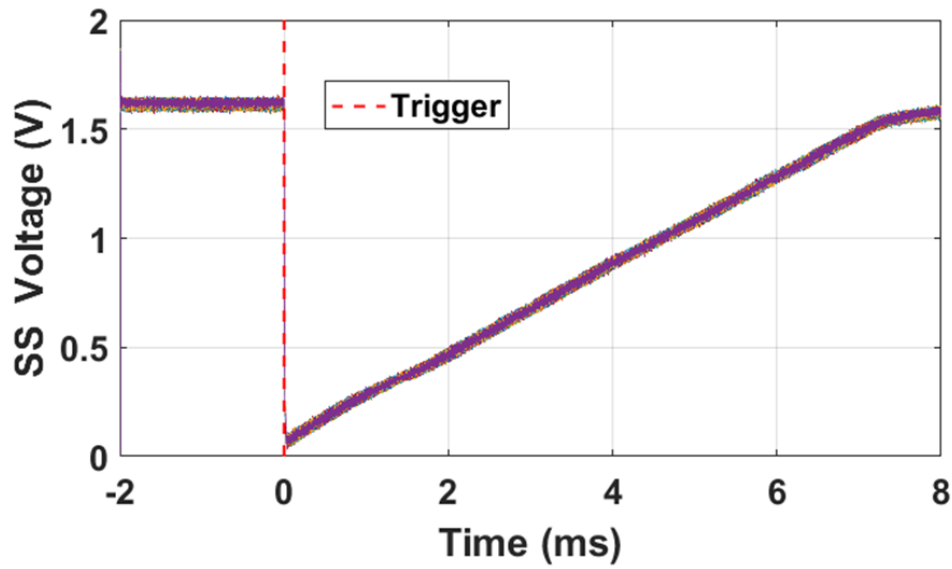
- (1) $V_{IN} = 5.0\text{ V}$, $V_{OUT} = 2.5\text{ V}$, and maximum load of 6 A, LET = 86.5 MeV-cm²/mg.
- (2) Soft-start duration is largely defined by the value soft-start capacitor. For these experiments $C_{SS} = 10\text{ nF}$. Using a lower value of C_{SS} can reduce the soft-star recovery time.

Figure 9. DPO Waveform Captures of V_{OUT} Overlay of 62 SEFI 2 Events in a TPS50601-SP



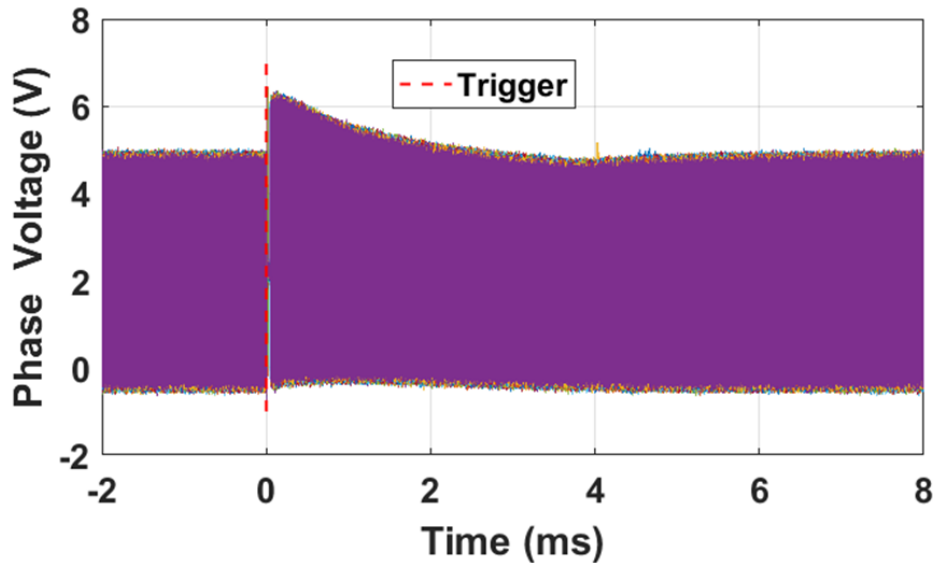
- (1) $V_{IN} = 5.0\text{ V}$, $V_{OUT} = 2.5\text{ V}$, and maximum load of 6 A, LET = 86.5 MeV-cm²/mg.
- (2) Soft-start duration is largely defined by the value soft-start capacitor. For these experiments $C_{SS} = 10\text{ nF}$. Using a lower value of C_{SS} can reduce the soft-star recovery time.

Figure 10. DPO Waveform Captures of P_{GOOD} Overlay of 62 SEFI 2 Events in a TPS50601-SP



- (1) Same 62 SEFI 2 events as [Figure 9](#) and [Figure 10](#).
- (2) Soft-start duration is largely defined by the value soft-start capacitor. For these experiments $C_{SS} = 10 \text{ nF}$. Using a lower value of C_{SS} can reduce the soft-start recovery time.

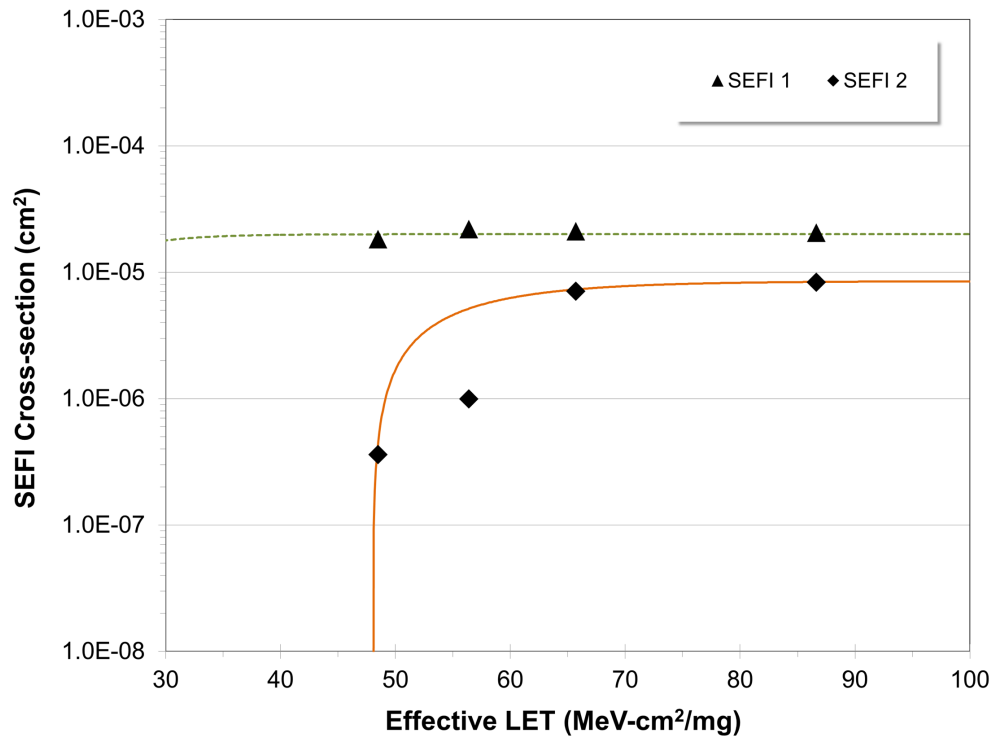
Figure 11. DPO Waveform Captures of Soft-Start (SS) Pin Response Overlay



- (1) Same 62 SEFI 2 events as [Figure 9](#) and [Figure 10](#).

Figure 12. DPO Waveform Captures of Phase (PH) Pin Overlay

SEFI cross-sections were obtained for the TPS50601-SP over more than a dozen trips to TAMU, several hundred heavy-ion runs, dozens of devices, at minimum to maximum V_{IN} , V_{OUT} , load conditions, at a range of ion fluxes and LET_{EFF} from 48.5 to 94.0 MeV-cm²/mg. This extensive SEE testing revealed that the highest LET-ions and maximum load condition resulted in the highest SEFI-rates. The SEFI cross-sections shown in Figure 13 were derived from a subset of all these tests and are a very good representation the SEFI performance of the TPS50601-SP. Four POL boards using the released PS50601SPEVM-D board design, and, to improve statistics, all tests were performed at a heavy ion fluence of 10⁷ ions/cm² with most of the tests repeated between 2 to 4 times for each condition. Even though only a few tests resulted in null-results or very low event counts, an upper bound was calculated based on a 95% confidence intervals as outlined in Appendix C. Table 5 summarizes the Weibull fit parameters for both SEFI 1 and SEFI 2 events.



- (1) $V_{IN} = 5.0$ V, $V_{OUT} = 2.5$ V, with maximum load of 6 A and with effective ion LETs ranging from 48.5 to 86.5 MeV-cm²/mg.

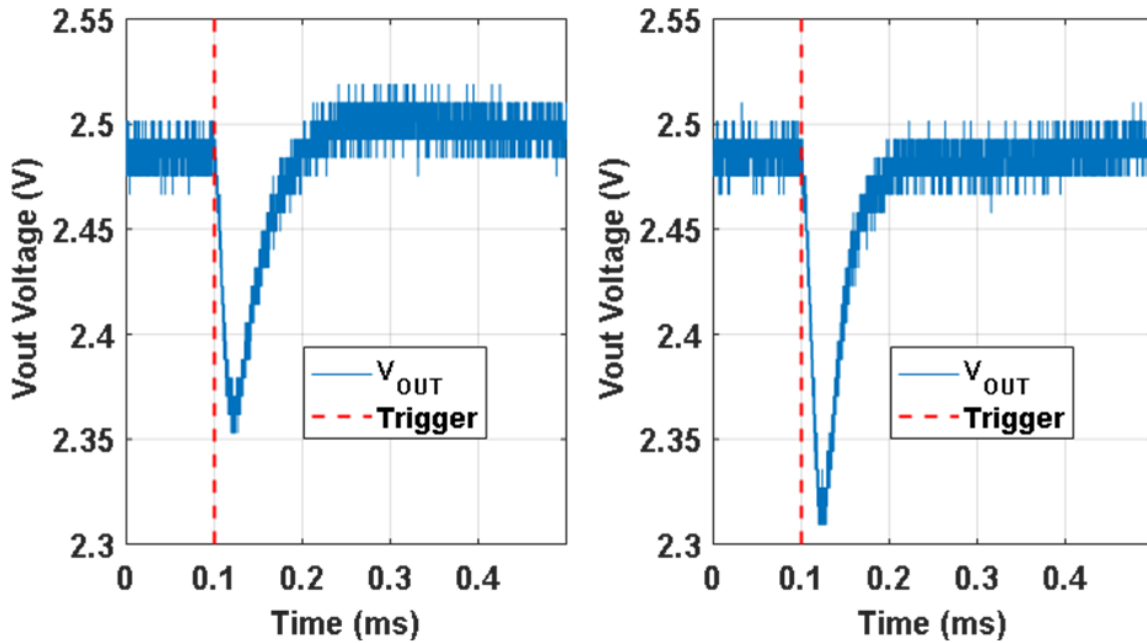
Figure 13. SEFI Cross-Section vs LET_{EFF} for TPS50601-SP

Table 5. Weibull Fitting Parameters for the SEFI Data

PARAMETER	SEFI 1	SEFI 2
Saturation cross-section	2.0E-05	8.5E-06
Onset LET	10.0	48.0
Width	9.0	9.0
Fitting	2.0	1.0

10 SET Results

SETs are defined as heavy-ion-induced transients on the V_{OUT} of the TPS50601-SP POL that were less than $\pm 9\%$ SETs on V_{OUT} . Events producing more than a 9% change in V_{OUT} induced a PGOOD transition and were thus categorized as SEFI 2 events as previously mentioned. All positive SETs (overshoots) were $< 5\%$ in magnitude and they all followed the standard recovery of a regulator from preceding negative SET events (undershoots). Thus overvoltage stress from SET is not an issue. The TPS50601-SP POL was SET-free for $LET_{EFF} < 65.3 \text{ MeV-cm}^2/\text{mg}$. A few SETs were observed at $65.7 \text{ MeV-cm}^2/\text{mg}$ which seemed to be the onset LET of the device. At $LET_{EFF} = 86.5 \text{ MeV-cm}^2/\text{mg}$ there were a larger number $> -5\%$ V_{OUT} events. Two maximal SETs are shown in Figure 14 for LET_{EFF} of 65.7 and $86.5 \text{ MeV-cm}^2/\text{mg}$ respectively.

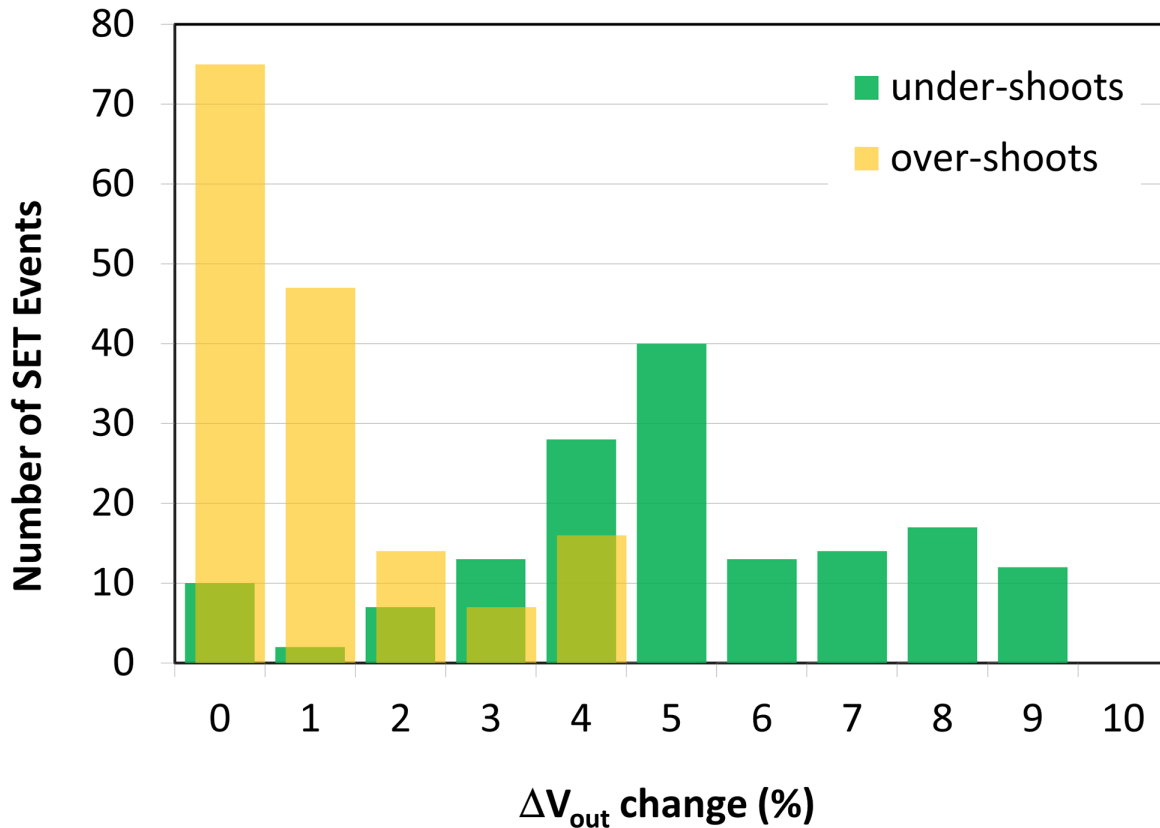


1. Observed from the TPS50601-SP at:
 - a. (Left) LET_{EFF} of $65.7 \text{ MeV-cm}^2/\text{mg}$ and,
 - b. (Right) Largest SET at an LET_{EFF} of $86.5 \text{ MeV-cm}^2/\text{mg}$.

Figure 14. The Worst-Case SET Events Captured by PXI

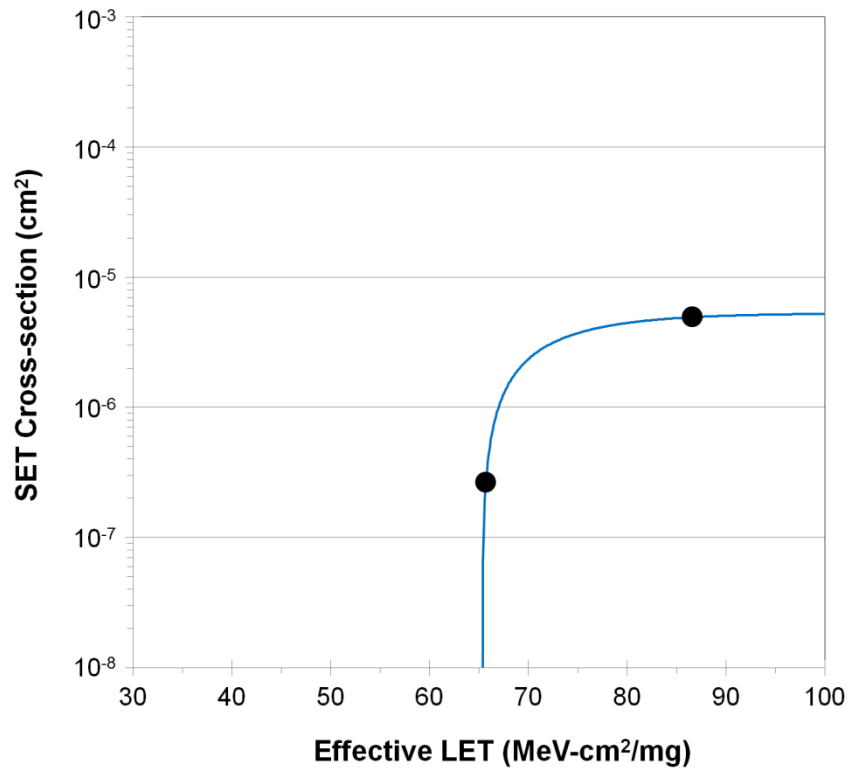
A histogram showing the total number of SETs binned as a function of the SET magnitude ($\% \Delta V_{OUT}$) is shown in Figure 15. The overshoots are shown in orange while the undershoots are shown in green. Clearly all overshoots are less than 5%. The SET cross-section shown in Figure 16 was obtained by extracting all SET events for the PXI waveform data base where ΔV_{OUT} of $> 5\%$ (just undershoots). An upper bound was calculated based on a 95% confidence interval (outlined in Appendix C).

Table 6 summarizes the Weibull fit parameters for the SET events. It is important to remember that SET in excess of 9-10% are not possible since events of this magnitude will trigger a valid P_{GOOD} signal to be generated (along with an automatic soft-start recovery), protecting down-stream components from the fluctuation – this type of event would be logged as a SEFI 2.



- (1) Overshoots (orange) and undershoots (green).
- (2) No SETs observed below LET = 65 MeV-cm²/mg.
- (3) All observed SETs were downward transients on V_{OUT} . Overshoots occurred during recovery from each event.
- (4) Each horizontal interval is 1% wide and in a given interval, 5 for example, represents $4\% \leq \Delta V_{OUT} < 5\%$.
- (5) All overshoots were $< 5\%$. Undershoots were more widely distributed with larger numbers of large events.

Figure 15. SET Histogram of Number of Events vs SET Magnitude (ΔV_{OUT})



- (1) $V_{IN} = 5.0\text{ V}$, $V_{OUT} = 2.5\text{ V}$, with maximum load of 6 A and with effective ion LETs ranging from 65.7 to 86.5 MeV-cm²/mg.

Figure 16. Cross-Section of SET events $V_O > 5\%$ vs LET_{EFF} for TPS50601-SP

Table 6. Weibull Fitting Parameters for SET Data

PARAMETER	SET
Saturation cross-section	5.3E-06
Onset LET	65.3
Width	16.0
Fitting	2.0

11 Event Rate Calculations

Event rates were calculated for LEO(ISS) and GEO environments by combining CREME96 orbital integral flux estimations and simplified SEE cross-sections according to methods described in [Appendix B](#). We assume a minimum shielding configuration of 100 mils (2.54 mm) of aluminum, and “worst-week” solar activity (this is similar to a 99% upper bound for the environment). Using the 95% upper-bounds for the SEL, SEFI 2, and SEL the event-rates of the TPS50601-SP are tabulated in [Table 7](#), [Table 8](#), [Table 9](#) respectively.

Table 7. SEL Event Rate Calculations for Worst-Week LEO and GEO Orbits

ORBIT TYPE	ONSET LET (MeV-cm ² /mg)	CREME96 INTEGRAL FLUX (/day-cm ²)	σ_{sat} (cm ²)	EVENT RATE (/day)	EVENT RATE (FIT)	MTBE (years)
LEO(ISS)	94.0	5.3E-07	3.7E-07	1.9E-13	8.1E-06	1.4E+10
GEO		1.4E-06		5.1E-13	2.1E-05	5.4E+09

Table 8. SEFI 2 Event Rate Calculations for Worst-Week LEO and GEO Orbits

ORBIT TYPE	ONSET LET (MeV-cm ² /mg)	CREME96 INTEGRAL FLUX (/day-cm ²)	σ_{sat} (cm ²)	EVENT RATE (/day)	EVENT RATE (FIT)	MTBE (years)
LEO(ISS)	48.0	4.5E-04	8.7E-06	3.9E-09	0.16	7.0E+05
GEO		1.5E-03		1.3E-08	0.53	2.1E+05

Table 9. SET Event Rate Calculations for Worst-Week LEO and GEO Orbits

ORBIT TYPE	ONSET LET (MeV-cm ² /mg)	CREME96 INTEGRAL FLUX (/day-cm ²)	σ_{sat} (cm ²)	EVENT RATE (/day)	EVENT RATE (FIT)	MTBE (years)
LEO(ISS)	65.3	1.1E-04	5.3E-06	6.0E-10	0.03	4.6E+06
GEO		3.2E-04		1.7E-09	0.07	1.6E+06

MTBE is the mean-time-between-events in years at the given event rates. These rates clearly demonstrate the SEE robustness of the TPS50601-SP POL in two harshly conservative space environments. Customers using the TPS50601-SP should only use the above estimations as a rough guide and we recommend that event rate calculations based on specific mission orbital and shielding parameters be performed to determine if the product will satisfy the reliability requirements for their specific mission.

12 Summary

The purpose of this study was to characterize the effect of heavy-ion irradiation on the single-event effect (SEE) performance of the TPS50601-SP synchronous step-down POL converter. Extensive SEE testing with heavy-ions having LET_{EFF} from 48.5 to 94.0 MeV-cm²/mg were conducted with heavy-ion fluences ranging from 1×10^6 to 1×10^7 ions/cm² per run, over a variety of input/output voltage conditions, load conditions, and two temperatures. The SEE results demonstrated that the TPS50601-SP POL is free of destructive SEB events and SEL-free up to $LET_{EFF} = 94.0$ MeV-cm²/mg. It is also SET free up to an LET of 65.3 MeV-cm²/mg and nearly SET-free up to $LET_{EFF} = 86.5$ MeV-cm²/mg. The TPS50601-SP has a relatively low recoverable SEFI saturation cross-section of $\sim 8.7 \times 10^{-6}$ at $LET_{EFF} = 86.5$ MeV-cm²/mg under maximum load and input/output voltage. CREME96-based worst-week event-rate calculations for LEO(ISS) and GEO orbits clearly demonstrate the robustness of the TPS50601-SP POL in two harshly conservative space environments.

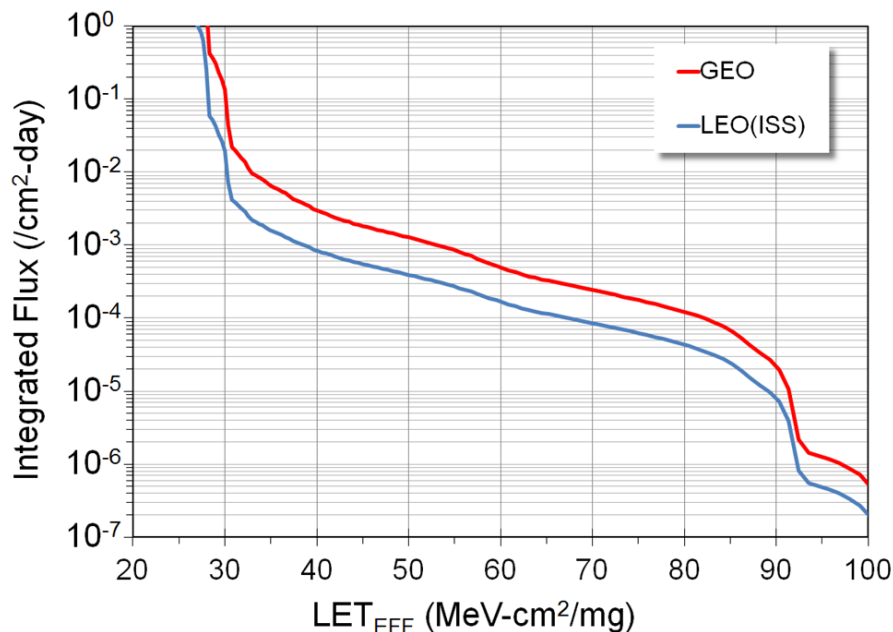
Total Ionizing Dose from SEE Experiments

The production TPS60501-SP POL is rated to a total ionizing dose (TID) of 100 krad(Si). In the course of the SEE testing, the heavy-ion exposures delivered ≈ 1 krad(Si) per 10^6 ions/cm² run. The cumulative TID exposure for each device respectively, over all runs they each underwent, was determined to be between 24 krad(Si) to 139 krad(Si). All nine production TPS60501-SP devices used in the studies described in this report stayed within specification and were fully-functional after the heavy-ion SEE testing was completed (with the exception of several units that were deliberately operated outside the SOA in an effort to capture the onset of SEB).

Orbital Environment Estimations

In order to calculate on-orbit SEE event rates one needs both the device SEE cross-section and the flux of particles encountered in a particular orbit. Device SEE cross-sections are usually determined experimentally while flux of particles in orbit is calculated using various codes. For the purpose of generating some event rates, a Low-Earth Orbit (LEO) and a Geostationary-Earth Orbit (GEO) were calculated using CREME96. CREME96 code, short for Cosmic Ray Effects on Micro-Electronics is a suite of programs [15][16] that enable estimation of the radiation environment in near-Earth orbits. CREME96 is one several tools available in the aerospace industry to provide accurate space environment calculations. Over the years since its introduction, the CREME models have been compared with on-orbit data and demonstrated their accuracy. In particular, CREME96 incorporates realistic “worst-case” solar particle event models, where fluxes can increase by several orders-of-magnitude over short periods of time.

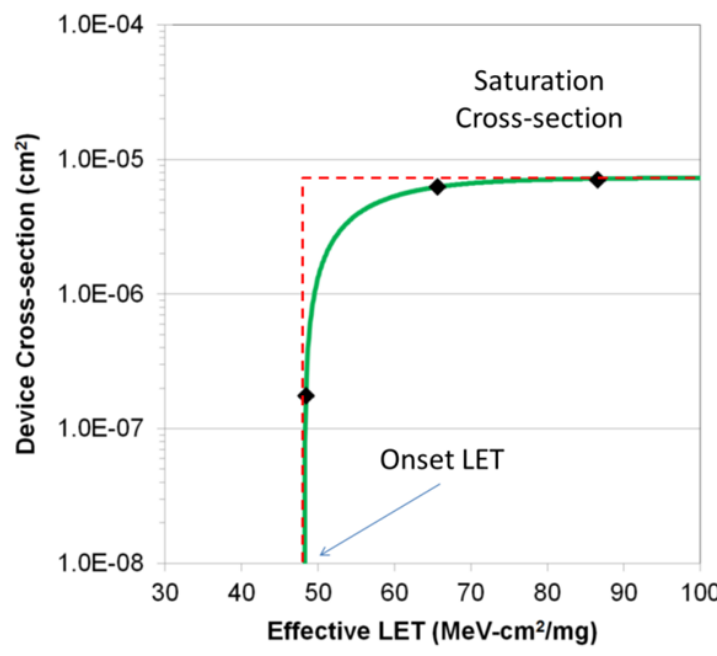
For the purposes of generating conservative event rates, the worst-week model (based on the biggest solar event lasting a week in the last 45 years) was selected, which has been equated to a 99%-confidence level worst-case event [17][18]. The integrated flux includes protons to heavy ions from solar and galactic sources. A minimal shielding configuration is assumed at 100 mils (2.54 mm) of aluminum. Two orbital environments were estimated, that of the International Space Station (ISS), which is LEO, and the GEO environment. Figure 17 shows the integrated flux (from high LET to low) for these two environments.



- (1) LEO(ISS) (blue) and a GEO (red) environment as calculated by CREME96 assuming worst-week and 100 mils (2.54 mm) of aluminum shielding.

Figure 17. Integral Particle Flux vs LET_{EFF}

Using this data, we can extract integral particle fluxes for any arbitrary LET of interest. To simplify the calculation of event rates we assume that all cross-section curves are square – meaning that below the onset LET the cross-section is identically zero while above the onset LET the cross-section is uniformly equal to the saturation cross-section. Figure 18 illustrates the approximation, with the green curve being the actual Weibull fit to the data with the “square” approximation shown as the red-dashed line. This allows us to calculate event rates with a single multiplication, the event rate becoming simply the product of the integral flux at the onset LET, and the saturation cross-section. Obviously this leads to an over-estimation of the event rate since the area under the square approximation is larger than the actual cross-section curve – but for the purposes of calculating upper-bound event rate estimates, this modification avoids the need to do the integral over the flux and cross-section curves.



(1) Weibull Fit (green) is “simplified” with the use of a square approximation (red dashed line).

Figure 18. Device Cross-Section vs LET_{EFF}

To demonstrate how the event rates in this report were calculated, assume that we wish to calculate an event rate for a GEO orbit for the device whose cross-section is shown in Figure 18. Using the red curve in Figure 17 and the onset LET value obtained from Figure 18 (~ 47 MeV-cm²/mg) we find the GEO integral flux to be ~ 1.6 × 10⁻³ ions/cm²-day. The event rate is the product of the integral flux and the saturation cross-section in Figure 16 (~ 7.5 × 10⁻⁶ cm²):

$$GEO \text{ Event Rate} = \left(1.6 \times 10^{-3} \frac{\text{ions}}{\text{cm}^2 \times \text{day}} \right) \times \left(7.5 \times 10^{-6} \text{ cm}^2 \right) = 1.2 \times 10^{-8} \frac{\text{events}}{\text{day}} \quad (3)$$

$$GEO \text{ Event Rate} = 5.0 \times 10^{-10} \frac{\text{events}}{\text{hr}} = 0.5 \text{ FIT} \quad (4)$$

$$MTBF = 234,000 \text{ Years!} \quad (5)$$

Confidence Interval Calculations

For conventional products where hundreds of failures are seen during a single exposure, one can determine the average failure rate of parts being tested in a heavy-ion beam as a function of fluence with high degree of certainty and reasonably tight standard deviation, and thus have a good deal of confidence that the calculated cross-section is accurate.

With radiation hardened parts however, determining the cross-section becomes more difficult since often few, or even, no failures are observed during an entire exposure. Determining the cross-section using an average failure rate with standard deviation is no longer a viable option, and the common practice of assuming a single error occurred at the conclusion of a null-result can end up in a greatly underestimated cross-section.

In cases where observed failures are rare or non-existent, the use of confidence intervals and the chi-squared distribution is indicated. The Chi-Squared distribution is particularly well-suited for the determination of a reliability level when the failures occur at a constant rate. In the case of SEE testing, where the ion events are random in time and position within the irradiation area, one expects a failure rate that is independent of time (presuming that parametric shifts induced by the total ionizing dose do not affect the failure rate), and thus the use of chi-squared statistical techniques is valid (since events are rare an exponential or Poisson distribution is usually used).

In a typical SEE experiment, the device-under-test (DUT) is exposed to a known, fixed fluence (ions/cm²) while the DUT is monitored for failures. This is analogous to fixed-time reliability testing and, more specifically, time-terminated testing, where the reliability test is terminated after a fixed amount of time whether or not a failure has occurred (in the case of SEE tests fluence is substituted for time and hence it is a fixed fluence test) [19]. Calculating a confidence interval specifically provides a range of values which is likely to contain the parameter of interest (the actual number of failures/fluence). Confidence intervals are constructed at a specific confidence level. For example, a 95% confidence level implies that if a given number of units were sampled numerous times and a confidence interval estimated for each test, the resulting set of confidence intervals would bracket the true population parameter in about 95% of the cases.

In order to estimate the cross-section from a null-result (no fails observed for a given fluence) with a confidence interval, we start with the standard reliability determination of lower-bound (minimum) mean-time-to-failure for fixed-time testing (an exponential distribution is assumed):

$$MTTF = \frac{2nT}{\chi^2_{2(d+1); 100\left(1-\frac{\alpha}{2}\right)}} \tag{6}$$

Where *MTTF* is the minimum (lower-bound) mean-time-to-failure, *n* is the number of units tested (presuming each unit is tested under identical conditions) and *T*, is the test time, and χ^2 is the chi-square distribution evaluated at 100 (1 – σ / 2) confidence level and where *d* is the degrees-of-freedom (the number of failures observed). With slight modification for our purposes we invert the inequality and substitute *F* (fluence) in the place of *T*:

$$MFTF = \frac{2nF}{\chi^2_{2(d+1); 100\left(1-\frac{\alpha}{2}\right)}} \tag{7}$$

Where now *MFTF* is mean-fluence-to-failure and *F* is the test fluence, and as before, χ^2 is the chi-square distribution evaluated at 100 $(1 - \sigma / 2)$ confidence and where *d* is the degrees-of-freedom (the number of failures observed). The inverse relation between MTTF and failure rate is mirrored with the MFTF. Thus the upper-bound cross-section is obtained by inverting the MFTF:

$$\sigma = \frac{\chi^2_{2(d+1); 100\left(1-\frac{\sigma}{2}\right)}}{2nF} \quad (8)$$

Let's assume that all tests are terminated at a total fluence of 10^6 ions/cm². Let's also assume that we have a number of devices with very different performances that are tested under identical conditions. Assume a 95% confidence level ($\sigma = 0.05$). Note that as *d* increases from 0 events to 100 events the actual confidence interval becomes smaller, indicating that the range of values of the true value of the population parameter (in this case the cross-section) is approaching the mean value + 1 standard deviation. This makes sense when one considers that as more events are observed the statistics are improved such that uncertainty in the actual device performance is reduced.

Table 10. Experimental Example Calculation of Mean-Fluence-to-Failure (MFTF) and σ Using a 95% Confidence Interval⁽¹⁾

Degrees-of-Freedom (d)	2(d + 1)	χ^2 @ 95%	Calculated Cross-Section (cm ²)		
			Upper-Bound @ 95% Confidence	Mean	Average + Standard Deviation
0	2	7.38	3.69E-06	0.00E+00	0.00E+00
1	4	11.14	5.57E-06	1.00E-06	2.00E-06
2	6	14.45	7.22E-06	2.00E-06	3.41E-06
3	8	17.53	8.77E-06	3.00E-06	4.73E-06
4	10	20.48	1.02E-05	4.00E-06	6.00E-06
5	12	23.34	1.17E-05	5.00E-06	7.24E-06
10	22	36.78	1.84E-05	1.00E-05	1.32E-05
50	102	131.84	6.59E-05	5.00E-05	5.71E-05
100	202	243.25	1.22E-04	1.00E-04	1.10E-04

⁽¹⁾ Using a 99% confidence for several different observed results (d = 0, 1, 2, and 3 observed events during fixed-fluence tests) on four identical devices and test conditions.

References

1. G. H. Johnson, R. D. Schrimpf, K. F. Galloway, and R. Koga, "Temperature dependence of single-event burnout in n-channel power MOSFETs [for space application]," *IEEE Trans. Nucl. Sci.*, 39(6), Dec. 1992, pp. 1605-1612.
2. D. K. Nichols, J. R. Coss, and K. P. McCarty, "Single event gate rupture in commercial power MOSFETs," *Radiation and its Effects on Components and Systems*, Sept. 1993, pp. 462 – 467.
3. M. Shoga and D. Binder, "Theory of Single Event Latchup in Complementary Metal-Oxide Semiconductor ICs", *IEEE Trans. Nucl. Sci.*, 33(6), Dec. 1986, pp. 1714-1717.
4. G. Bruguier and J.M. Palau, "Single particle-induced latchup", *IEEE Trans. Nucl. Sci.*, Vol. 43(2), Mar. 1996, pp. 522-532.
5. J. M. Hutson, R. D. Schrimpf, and L. W. Massengill, "The effects of scaling and well and substrate contact placement on single event latchup in bulk CMOS technology," in *Proc. RADECS*, Sept. 2005, pp. PC24-1–PC24-5.
6. N. A. Dodds, J. M. Hutson, J. A. Pellish, et al., "Selection of Well Contact Densities for Latchup-Immune Minimal-Area ICs, *IEEE Trans. Nucl. Sci.*, Vol. 57(6), Dec. 2010, pp. 3575-3581.
7. D. B. Estreich and A. Ochoa, Jr., and R. W. Dutton, "An Analysis of Latch-Up Prevention in CMOS IC's Using an Epitaxial-Buried Layer Process", *Proceed. IEEE Elec. Dev. Meeting*, 24, Dec. 1978, pp. 230-234.
8. R. Krithivasan, et al., "Application of RHBD techniques to SEU hardening of Third-Generation SiGe HBT Logic Circuits," *IEEE Trans. Nucl. Sci.* Vol. 53(6), Dec. 2006, pp. 3400-3407.
9. P. C. Adell, R. D. Schrimpf, B. K. Choi, W. T. Holman, J. P. Attwood, C. R. Cirba, and K. F. Galloway, "Total-Dose and Single-Event Effects in Switching DC/DC Power Converters," *IEEE Trans. Nucl. Sci.* Vol. 49(6), Dec. 2002, pp. 3217-3221.
10. R. L. Pease, "Modeling Single Event Transients in Bipolar Linear Circuits," *IEEE Trans. Nucl. Sci.* vol. 55(4), Aug. 2008, pp. 1879-1890.
11. R. Lveugle and A. Ammari, "Early SEU Fault Injection in Digital, Analog and Mixed Signal Circuits: a Global Flow," *Proc. of Design, Automation and Test in Europe Conf.*, 2004, pp. 1530-1591.
12. P. C. Adell, R. D. Schrimpf, B. K. Choi, W. T. Holman, J. P. Attwood, C. R. Cirba, and K. F. Galloway, "Total-Dose and Single-Event Effects in Switching DC/DC Power Converters," *IEEE Trans. Nucl. Sci.* Vol. 49(6), Dec. 2002, pp. 3217-3221.
13. TAMU Radiation Effects Facility website. <http://cyclotron.tamu.edu/ref/>
14. "The Stopping and Range of Ions in Matter" (SRIM) software simulation tools website. <http://www.srim.org/index.htm#SRIMMENU>
15. <https://creme.isde.vanderbilt.edu/CREME-MC>
16. A. J. Tylka, et al., "CREME96: A Revision of the Cosmic Ray Effects on Micro-Electronics Code", *IEEE Trans. Nucl. Sci.*, 44(6), 1997, pp. 2150-2160.
17. A. J. Tylka, W. F. Dietrich, and P. R. Bobery, "Probability distributions of high-energy solar-heavy-ion fluxes from IMP-8: 1973-1996", *IEEE Trans. on Nucl. Sci.*, 44(6), Dec. 1997, pp. 2140 – 2149.
18. A. J. Tylka, J. H. Adams, P. R. Bobery, et al., "CREME96: A Revision of the Cosmic Ray Effects on Micro-Electronics Code", *Trans. on Nucl. Sci.*, 44(6), Dec. 1997, pp. 2150 – 2160.
19. D. Kececioglu, "Reliability and Life Testing Handbook", Vol. 1, PTR Prentice Hall, New Jersey, 1993, pp. 186-193.

IMPORTANT NOTICE FOR TI DESIGN INFORMATION AND RESOURCES

Texas Instruments Incorporated ("TI") technical, application or other design advice, services or information, including, but not limited to, reference designs and materials relating to evaluation modules, (collectively, "TI Resources") are intended to assist designers who are developing applications that incorporate TI products; by downloading, accessing or using any particular TI Resource in any way, you (individually or, if you are acting on behalf of a company, your company) agree to use it solely for this purpose and subject to the terms of this Notice.

TI's provision of TI Resources does not expand or otherwise alter TI's applicable published warranties or warranty disclaimers for TI products, and no additional obligations or liabilities arise from TI providing such TI Resources. TI reserves the right to make corrections, enhancements, improvements and other changes to its TI Resources.

You understand and agree that you remain responsible for using your independent analysis, evaluation and judgment in designing your applications and that you have full and exclusive responsibility to assure the safety of your applications and compliance of your applications (and of all TI products used in or for your applications) with all applicable regulations, laws and other applicable requirements. You represent that, with respect to your applications, you have all the necessary expertise to create and implement safeguards that (1) anticipate dangerous consequences of failures, (2) monitor failures and their consequences, and (3) lessen the likelihood of failures that might cause harm and take appropriate actions. You agree that prior to using or distributing any applications that include TI products, you will thoroughly test such applications and the functionality of such TI products as used in such applications. TI has not conducted any testing other than that specifically described in the published documentation for a particular TI Resource.

You are authorized to use, copy and modify any individual TI Resource only in connection with the development of applications that include the TI product(s) identified in such TI Resource. NO OTHER LICENSE, EXPRESS OR IMPLIED, BY ESTOPPEL OR OTHERWISE TO ANY OTHER TI INTELLECTUAL PROPERTY RIGHT, AND NO LICENSE TO ANY TECHNOLOGY OR INTELLECTUAL PROPERTY RIGHT OF TI OR ANY THIRD PARTY IS GRANTED HEREIN, including but not limited to any patent right, copyright, mask work right, or other intellectual property right relating to any combination, machine, or process in which TI products or services are used. Information regarding or referencing third-party products or services does not constitute a license to use such products or services, or a warranty or endorsement thereof. Use of TI Resources may require a license from a third party under the patents or other intellectual property of the third party, or a license from TI under the patents or other intellectual property of TI.

TI RESOURCES ARE PROVIDED "AS IS" AND WITH ALL FAULTS. TI DISCLAIMS ALL OTHER WARRANTIES OR REPRESENTATIONS, EXPRESS OR IMPLIED, REGARDING TI RESOURCES OR USE THEREOF, INCLUDING BUT NOT LIMITED TO ACCURACY OR COMPLETENESS, TITLE, ANY EPIDEMIC FAILURE WARRANTY AND ANY IMPLIED WARRANTIES OF MERCHANTABILITY, FITNESS FOR A PARTICULAR PURPOSE, AND NON-INFRINGEMENT OF ANY THIRD PARTY INTELLECTUAL PROPERTY RIGHTS.

TI SHALL NOT BE LIABLE FOR AND SHALL NOT DEFEND OR INDEMNIFY YOU AGAINST ANY CLAIM, INCLUDING BUT NOT LIMITED TO ANY INFRINGEMENT CLAIM THAT RELATES TO OR IS BASED ON ANY COMBINATION OF PRODUCTS EVEN IF DESCRIBED IN TI RESOURCES OR OTHERWISE. IN NO EVENT SHALL TI BE LIABLE FOR ANY ACTUAL, DIRECT, SPECIAL, COLLATERAL, INDIRECT, PUNITIVE, INCIDENTAL, CONSEQUENTIAL OR EXEMPLARY DAMAGES IN CONNECTION WITH OR ARISING OUT OF TI RESOURCES OR USE THEREOF, AND REGARDLESS OF WHETHER TI HAS BEEN ADVISED OF THE POSSIBILITY OF SUCH DAMAGES.

You agree to fully indemnify TI and its representatives against any damages, costs, losses, and/or liabilities arising out of your non-compliance with the terms and provisions of this Notice.

This Notice applies to TI Resources. Additional terms apply to the use and purchase of certain types of materials, TI products and services. These include; without limitation, TI's standard terms for semiconductor products (<http://www.ti.com/sc/docs/stdterms.htm>), [evaluation modules](#), and [samples](http://www.ti.com/sc/docs/sampterm.htm) (<http://www.ti.com/sc/docs/sampterm.htm>).

Mailing Address: Texas Instruments, Post Office Box 655303, Dallas, Texas 75265
Copyright © 2017, Texas Instruments Incorporated